



HAL
open science

First Step Towards a Fully-Miniaturized Intra-Body Communication Transceiver Based on Galvanic Coupling

Stéphane Pitou, Tristan Rouyer, Sylvain Bonhommeau, Serge Bernard, Fabien Soulier, Vincent Kerzérho

► **To cite this version:**

Stéphane Pitou, Tristan Rouyer, Sylvain Bonhommeau, Serge Bernard, Fabien Soulier, et al.. First Step Towards a Fully-Miniaturized Intra-Body Communication Transceiver Based on Galvanic Coupling. FICC 2023 - Future of Information and Communication Conference, Mar 2023, San Francisco (Virtual), United States. pp.107-119, 10.1007/978-3-031-28076-4_11 . lirmm-03866901

HAL Id: lirmm-03866901

<https://hal-lirmm.ccsd.cnrs.fr/lirmm-03866901v1>

Submitted on 23 Nov 2022

HAL is a multi-disciplinary open access archive for the deposit and dissemination of scientific research documents, whether they are published or not. The documents may come from teaching and research institutions in France or abroad, or from public or private research centers.

L'archive ouverte pluridisciplinaire **HAL**, est destinée au dépôt et à la diffusion de documents scientifiques de niveau recherche, publiés ou non, émanant des établissements d'enseignement et de recherche français ou étrangers, des laboratoires publics ou privés.

First Step Towards a Fully-Miniaturized Intra-Body Communication Transceiver Based on Galvanic Coupling

Stéphane Pitou¹, Tristan Rouyer², Sylvain Bonhommeau³, Serge Bernard¹, Fabien Soulier¹, and Vincent Kerzérho¹

¹ LIRMM, Univ Montpellier, CNRS, Montpellier, France

² MARBEC, Univ Montpellier, CNRS, IFREMER, IRD, Montpellier, France

³ IFREMER, DOI, Le Port, France

contact: stephane.pitou@lirmm.fr, vincent.kerzerho@lirmm.fr

Abstract. With the growing interest in wireless medical implants, efficient and secure intra-body communication becomes mandatory. A promising technique is the Galvanic Coupling (GC) communication. This research area is in constant evolution but despite this, currently there is no complete miniaturized transceiver architecture solution proposed in the literature. In this paper, we present the first fully-miniaturized GC transceiver architecture based on off-the-shelf components considering implantability constraints such as size and power consumption. The transmitter consists of a micro-controller, a Direct Digital Synthesizer (DDS) for analog sine wave generation and an amplifier. The receiver is made of a two-stage analog amplification chain. The first stage is a instrumentation amplifier and the second stage is made of a operational amplifier (Op Amp). Two versions of the receiver has been designed with two instrumentation amplifiers. The design has been tested using a phantom, in a on-body to on-body and an implanted to implanted configurations. The proposed architecture is a compromise between implantation constraints (components area of 0.75 cm² and maximum consumption 18 mA) and maximum transmission frequency (800 kHz). The intra-body communication has been validated for various distances (up to 60 cm), four different electrodes relative orientations and in different settings (on body and intra-body).

...

Keywords: body area network, galvanic coupling, intra-body communication, transceiver

1 Introduction

Human body communication is a research topic that has gained interest with the development of active medical implants and the need for dedicated communication techniques in a context of implanted sensor network. A promising solution is the galvanic coupling (GC) communication. The basic principle consists in

using biological tissue as a medium for modulated electrical signals. The signal is transmitted and received through the tissue using two pairs of electrodes. GC is a strong competitor to obvious solution, that is radio-frequency (RF) communication technique. Indeed GC has several advantages. At first, it is a secured technique as the transmission channel is limited to the body, on contrary to RF communications which can be received by any system close enough to the transmitter. Then, GC doesn't need for antenna. It is a significant benefit compare to RF, because antenna size Vs efficiency trade-off can be a challenge considering active implant application. In addition as mentioned in [1], it is commonly assumed that GC is less power consuming because it doesn't need for same power greedy components as for RF designs.

A main topic related to GC is the finite-element modeling and simulation of the communication channel, which is the human body [2, 3]. These works aim at estimating the impact of body composition by differentiating conductivity and permittivity of its various constitutive elements such as blood, bone, skin, muscle and fat on the communication performances, such as path loss. We can also find in the literature several works related to the communication protocol definition according to the GC application [4]. In addition the effect of electrodes positioning based on vertical and horizontal dipoles is also studied [5–7]. From hardware implementation point, [4, 6] propose two designs of GC transceivers using off-the-shelf components but these designs are not made considering implantable constraints such as size and power consumption. [1, 8] present the most advanced research developments as they describe some implantable designs. [8] presents a high data-rate capsule for endoscopy as [1] introduces an innovative galvanic impulse link. Both designs have been done for intra-body communication resulting in small and low-power systems. In addition they have been validated intra-body. It has to be noticed that the implanted systems are only transmitters. The receiver part has not been implemented probably because it isn't useful for the application or maybe to reduce the size and consumption of the whole systems.

This publication introduces the first fully-miniaturized transceiver architecture based on off-the-shelf components for multi case studies of intra-body communication (implanted to on-body, on-body to implanted, on-body to on-body, implanted to implanted) in order to make it implantable while targeting the higher communication frequency to increase the data rate. The second section is the materials and methods section, presenting the proposed transceiver architecture and the validation protocols. Tests and validation results are presented in the third section. As the fourth section proposes a discussion on the results and more generally the topic of implantable GC transceiver.

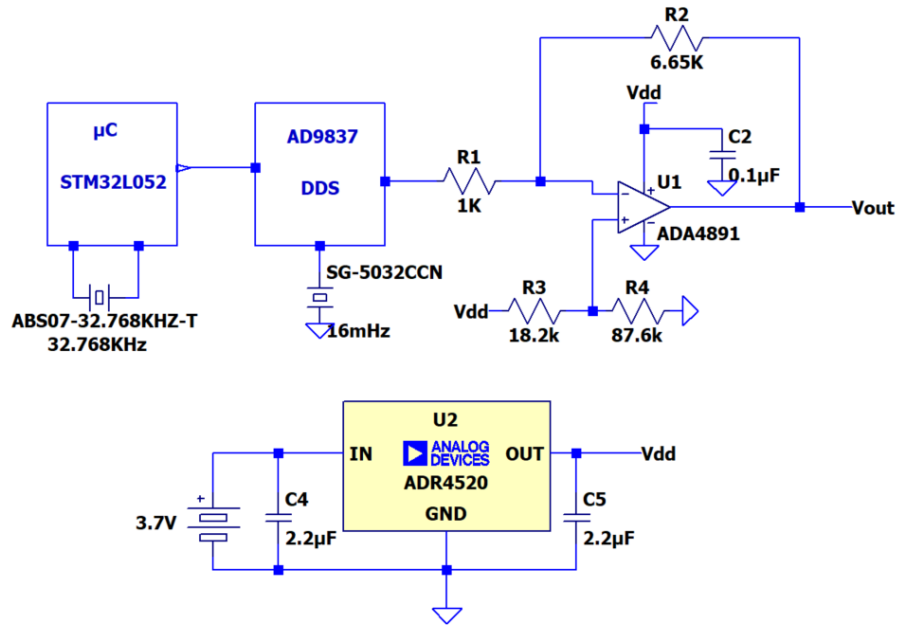


Fig. 1. Transmission (Tx) architecture.

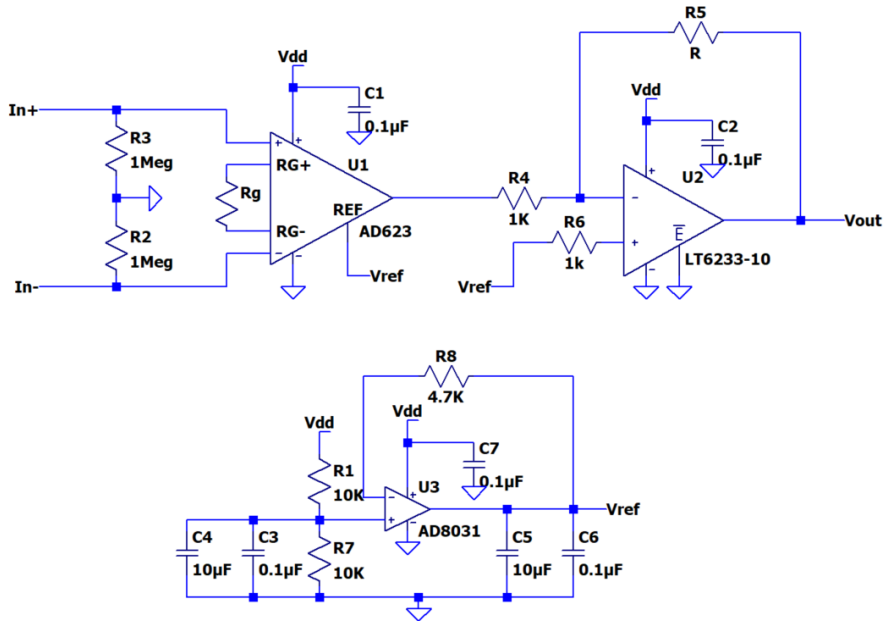


Fig. 2. Receiver (Rx) architecture.

2 Materials and methods

2.1 Transceiver Architecture

In order to design an implantable transceiver using off-the-shelf components, it is mandatory to have the smallest and less consuming components and the smallest number of components for limiting size and power consumption.

The transmitter architecture is given by “Fig. 1”. It is composed of digital and analog parts. The analog sinewave is generated by a Direct Digital Synthesizer (DDS). DDS enables to generate various sinewave frequencies from 1Hz to few MHz. Few modulation types can also be implemented using a DDS, such as frequency, phase or amplitude modulations. The smallest DDS (AD9837, 10 Lead LFCSP $3 \times 3\text{mm}$) with a 16MHz oscillator has been chosen for our architecture. The DDS needs to be driven by a micro-controller. For size and power consumption considerations, the choice fell on one of the STM32 low power family, with relatively small amount of memory and small functioning frequency (STM32L051T6Y6, 32kB and 32MHz, $88\mu\text{A MHz}^{-1}$). In addition the smallest package has been chosen (WLCSP $2.6 \times 2.8\text{mm}$). This component will drive the DDS to change its frequency. Again, for reduced number of components, a single supply has been chosen. The Tx board is battery powered at 3.3V through a regulator and all are powered by a 3.7V lithium battery in order to have a ground dissociation from earth ground. The DDS output amplitude is only 0.6Vpp, so an Operational Amplifier (Op Amp) has been implemented to rise it to 3.2Vpp. The Op Amp shall have a high bandwidth and high slew rate (ADA4891, 240MHz and $170\text{V } \mu\text{S}^{-1}$). The electrode is connected between Vout and the ground. The total area covered by components is 0.45 cm^2 .

The receiver architecture (“Fig. 2”) is only composed by analog components, as we assume in a whole transceiver system that the micro-controller is shared between Tx and Rx. It is a two-stage amplification. The gain settings is then noted as follow: (Gain 1; Gain 2), for example (2;100) for a global gain of 200. The first amplification stage is made of an Instrumentation Amplifier (In Amp). The gain of the In Amp is set by Rg resistor. The second amplification is done using a low noise Op Amp (LT6233-10, GBW 375MHz, 1.9nV Hz^{-2}). The output signal can be sampled by the Analog-to-Digital Converter (ADC) of the micro-controller. The Rx has also a single supply of 3.3V.

In Amp is a sensitive element of the whole system as it has to amplify a very small signal coming out of the biological tissue, while it is limited by its Gain-Bandwidth product (GBW). The selection criteria were the GBW, a single supply for operation around 3.3V, limited current consumption, availability and Common Mode Voltage needed. According to this criteria, two In Amp have been selected: AD623 from Analog Devices and INA823 from Texas Instrument. They are pin to pin compatible and correspond to our requirement. So it has been decided to test both components. The electrode is connected between In+ and In - of the In Amp. The In Amp need a reference voltage at $V_{cc}/2$. This voltage cannot be set with a simple voltage divider due to the internal schematics of the In Amp. With this method, the resistor will be taken into account by the In

Amp and downgrades is performance. The solution is to use a buffer (AD8031) between the voltage divider and the In Amp with some anti-parasitic capacitors. The total area covered by component for the Rx board is 0.30 cm^2 .

2.2 Test Methods

The tests have several purposes. At first Tx and Rx have been tested and characterized independently. Tx has been connected to an oscilloscope (Agilent DSO6014A) for functioning signal observation. Signal amplitude and power consumption have been measured for frequencies varying from 30kHz to 2MHz. For Rx testing, a signal generator (TTI TG5011) has been connected to its input. A 10mVpp-amplitude sinewave with a frequency varying from 1kHz to 2MHz has been provided to Rx. Rx output has been observed using an oscilloscope and the consumption measured using a current monitor (ST X-NUCLEO-LPM01A). According to the smallest amplitude of few mV that can be expected as Rx input signal, the Rx gain has been set to 200 ((2;100) or (1;200)) in order to obtain a signal of few hundreds of mV to 2V in order to make it high enough for post-processing without saturating Rx output. The total gain has been set to these values for the whole tests.

Then the next objective of experiments was to validate the feasibility of a GC communication using the whole proposed architecture. The third purpose was to set-up various hardware configurations to compare the two previously mentioned In Amps (AD623, INA823) and to characterize the system performances in terms of gain, noise and bandwidth. To reach these objectives, we have considered two measurement set-ups regularly described in the literature which are communication on a arm (“Fig.3”) and communication in a phantom. The phantom is made of tap water with 0.9% of Sodium Chloride (NaCl). To vary the conductivity, the tests have also been done using tap water without any added sodium. The phantom conductivity has been measured from 1kHz to 1MHz using Zurich Instruments impedance analyzer MFIA and the Gravity conductivity sensor from DFrobot (K=10).

In addition, as the long-term purpose of this study is the deployment of a sensor network implanted in a fish, two additional test configurations have been set up, a GC communication through a *Dicentrarchus labrax* (European sea Bass) and a GC communication through a and *Thunnus thynnus* (Bluefin tuna), they are respectively presented by “Fig. 4” and “Fig. 5” . Both communications can be assimilated to implant-to-implant communications as they have been done using implanted electrodes. Based on these additional tests, we have studied the possibility to communicate through fish muscles, the impact of electrodes relative orientation (“Fig.6”) and the distance between electrodes. The Rx output signals have been analyzed using an oscilloscope and a spectral analyzer (Analog Discovery 2 and Waveform software).

For on-body test, the electrode used is Covidien ECG electrodes ref : 31.1245.21. As presented in “Fig. 3”, the electrode pairs are separated by 20cm and have a distance between contacts of 4cm . Conductive gel has been used to ensure a good contact between electrode and skin. For the phantom and implanted-in-fish



Fig. 3. On-body to on-body GC communication on a arm.

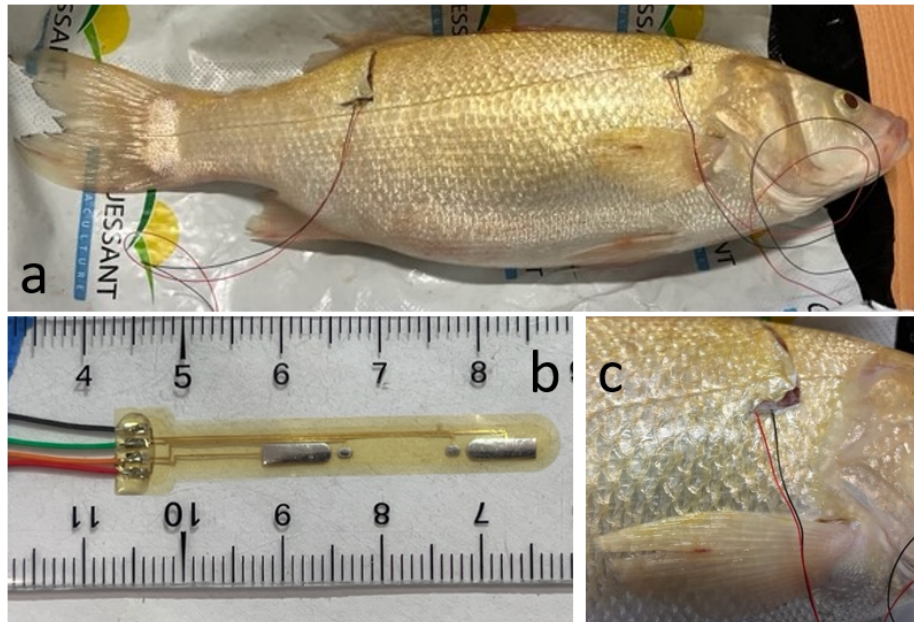


Fig. 4. a) GC communication in an European sea bass. b) Flexible electrode. c) Implanted electrode



Fig. 5. a) GC communication in a Bluefin Tuna. b) Tx implanted Electrode. c) Rx Implanted Electrode

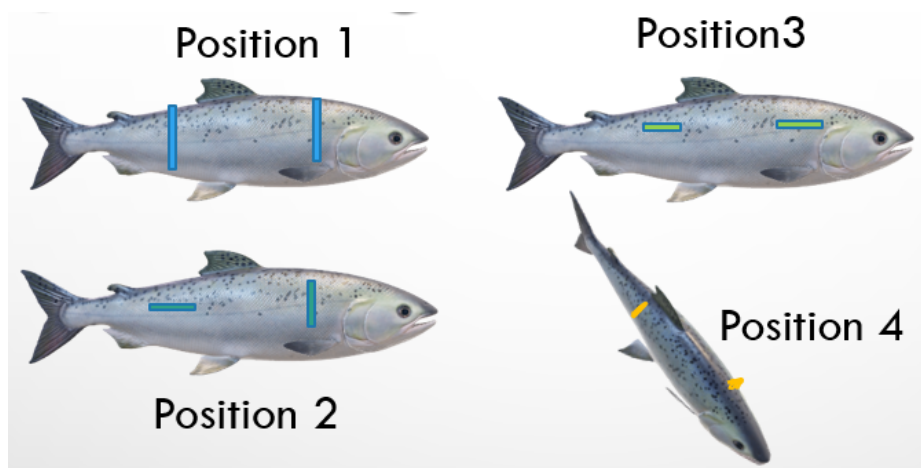


Fig. 6. Electrodes relative orientation, Tx on head side, Rx on tail side

tests, the electrode used is an implantable, bio-compatible, flexible electrode [9] developed for bio-impedance measurement application “Fig. 4b”. For GC communication, only the two bigger pads are used.

3 Results

3.1 Tx and Rx Independent Tests

Tx output signal has been measured at 3.2Vpp. The total consumption during a transmission is 15mA equally distributed between the micro-controller, the DDS and the Op Amp. “Fig. 7” presents the Rx gain in dB for the two In Amp and the two gain settings. We observe that INA823 has a largest bandwidth whatever the gain value.” Tab. 1” summarizes Rx characterization. The Rx power consumption includes the two amplification stages and the reference Op Amp consumptions. It appears that the consumption is independent of the frequency or gain selection.

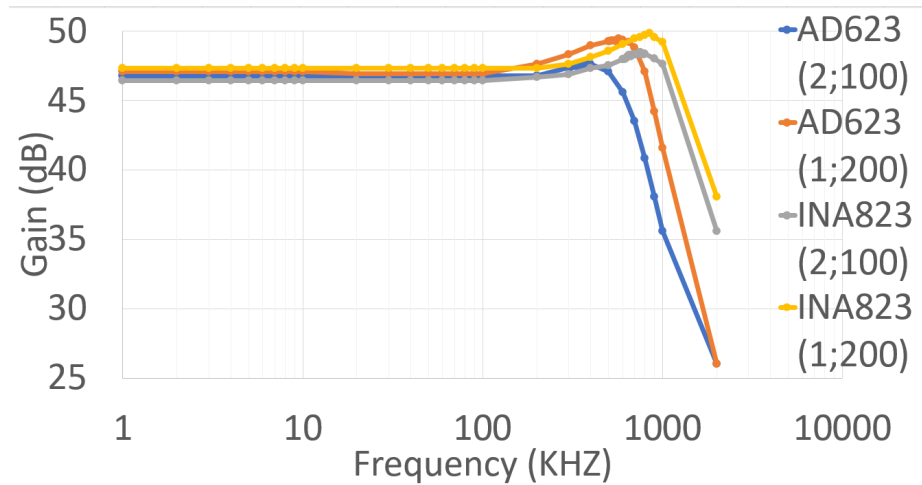


Fig. 7. Rx Gain Versus Frequency.

3.2 Through Arm GC Communication

AD623 has a better amplitude answer whereas INA823 still has a higher maximum gain frequency (“Fig. 8”). The path loss in the arm depends of the frequency. It varies from -71dBV @30kHz and -53dBV @600kHz.

Table 1. Rx characterization summary

Reference	In Amp Current consumption (μA)	Board Current consumption (mA)	Max Gain frequency (KHz)	Gain
AD623	435	2,4	570 380	1;200 2;100
INA823	305	2,47	800 750	1;200 2;100

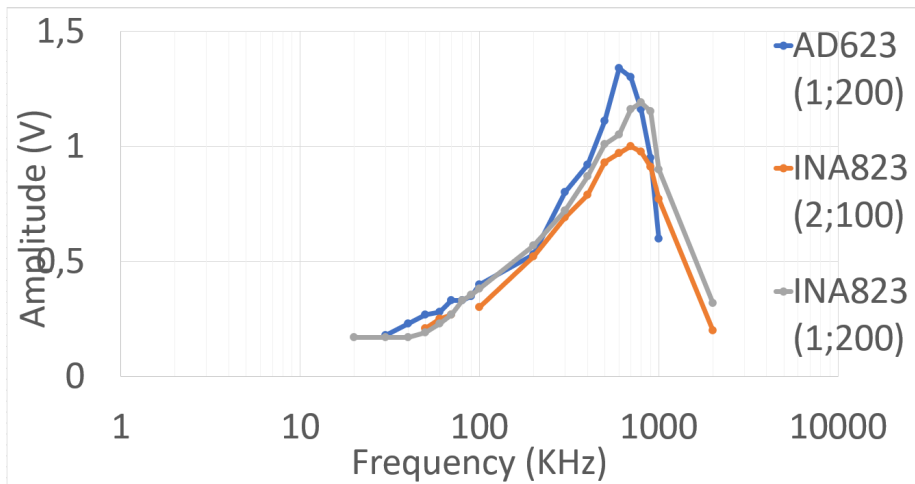


Fig. 8. Rx output signal amplitude in arm.

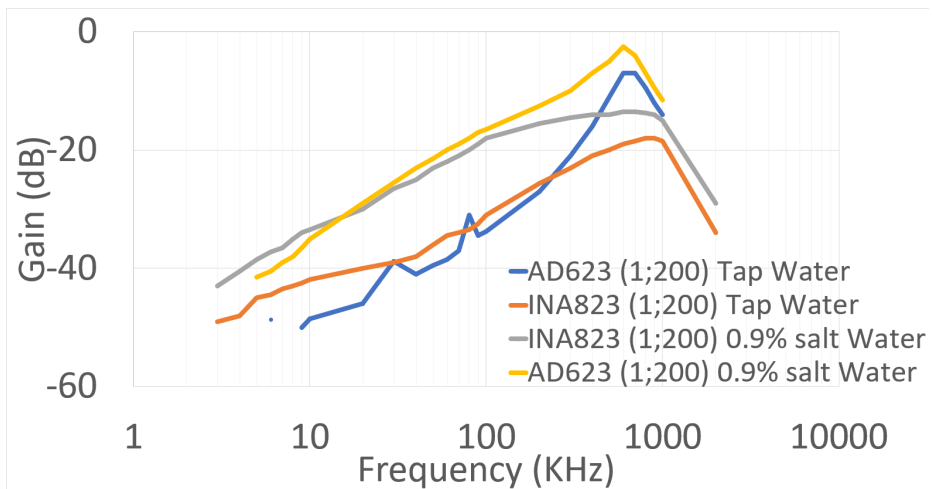


Fig. 9. Rx output signal gain in phantom

3.3 GC Communication in the Phantom

“Fig. 11” presents the conductivity of a buffer solution (12.88 mS cm^{-1} at 2.7kHz) and the phantom for tap water with and without added sodium, from 1kHz to 1MHz . Conductivity is frequency dependent. Tap water, according to the local legislation, has a conductivity lower than 1mS cm^{-1} at 2.7kHz and increases at higher frequency due to the naturally present ions. Adding 0.9% of Sodium Chloride (NaCl), conductivity increase and NaCl combined with present ion’s in tap water induces a higher conductivity in high frequency.

Test with this water (tap and salted) induced better results in upper frequencies. The noise parameter is the Signal to Noise Ratio (SNR). The noise decreases as frequency increases, so the result as the same profile than the gain (“Fig. 10”). The higher the frequency is, the better the performances are. The system gain and SNR reach their highest values at 600kHz for AD623 and 800kHz for INA823. “Fig. 9”

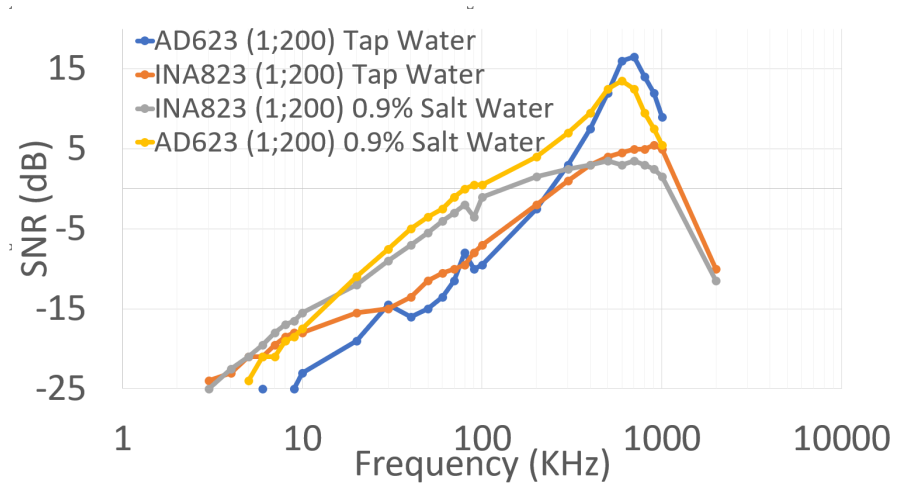


Fig. 10. Rx output signal SNR in phantom.

3.4 GC Communication in Fishes

European Sea Bass “Fig. 12” presents the Rx output signal after a (2;100) gain amplification using AD623 as an input In Amp, for four relative orientations of the electrodes. First of all, the GC communication is feasible in all the orientation cases. For the four cases, we observe an increase of the received signal amplitude with the increasing frequency. The maximum amplitude is still around 600kHz . Position 1 has a maximum amplitude of 1.7V , which is much higher than the other positions which have a maximum amplitude between 0.2

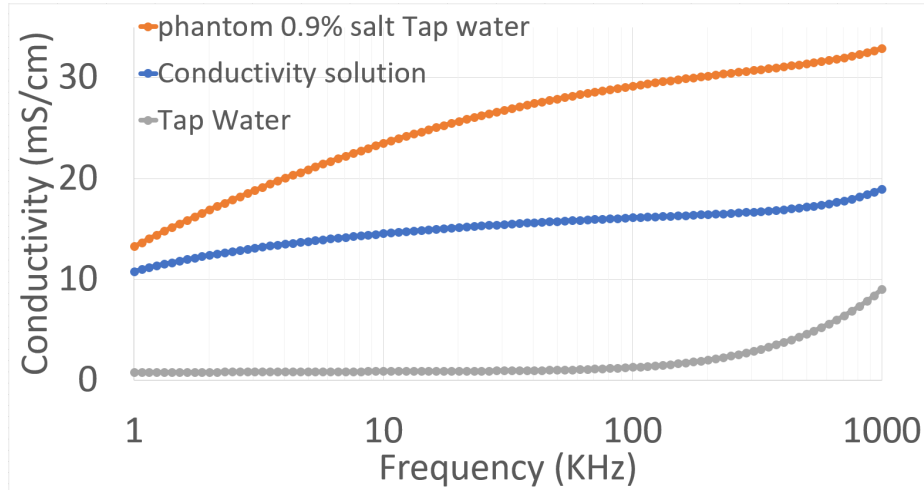


Fig. 11. Conductivity function of frequency for different type of liquid

and 0.5V. Assuming that it is because contacts of the two electrodes face each other and the electric field lines follow the muscle fibers which are known to be anisotropic.

Bluefin Tuna “Fig. 13” provides the test results for GC communication in a bluefin tuna. Two distances (20cm, 60cm) between electrodes have been tested with also two relative orientation (position 1, position 2) and two gain settings ((1;200),(2;100)). The first observation is that the GC communication is effective even at 60cm. We observe that the conductivity increases with increasing frequency. Like for the test on the European sea bass, the position 1 provides higher received signal amplitude. The signal amplitude compared to the previous fish, at 20cm, in same electrode position is higher in the bluefin tuna. The conclusion about that is at a same frequency, distance and position, the conductivity is better in the tuna than in the European sea bass. So we assume that the conductivity value varies according to the species.

4 Discussion

The initial purpose of this study was to design the first GC transceiver using off-the-shelf components for implant to implant, implant to on-body and on-body to on-body communications. In order to reach this first and main objective, it is mandatory to limit the number and size of components as the size and consumption of the whole system. The total components area is 0.75cm^2 . Regarding the whole transceiver size, we currently work on the design of the board and we assume to obtain an area around 3cm^2 which allows to expect the system to be implanted.

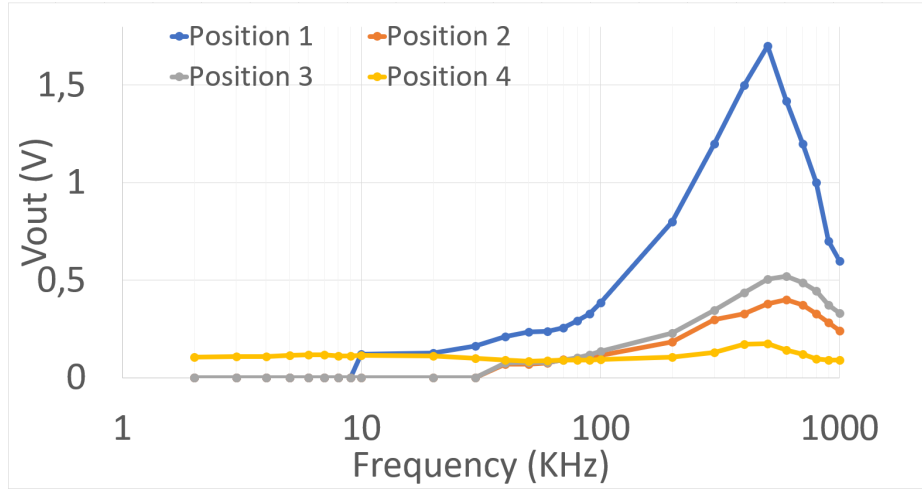


Fig. 12. Output Rx signal amplitude on a sea bass in different position

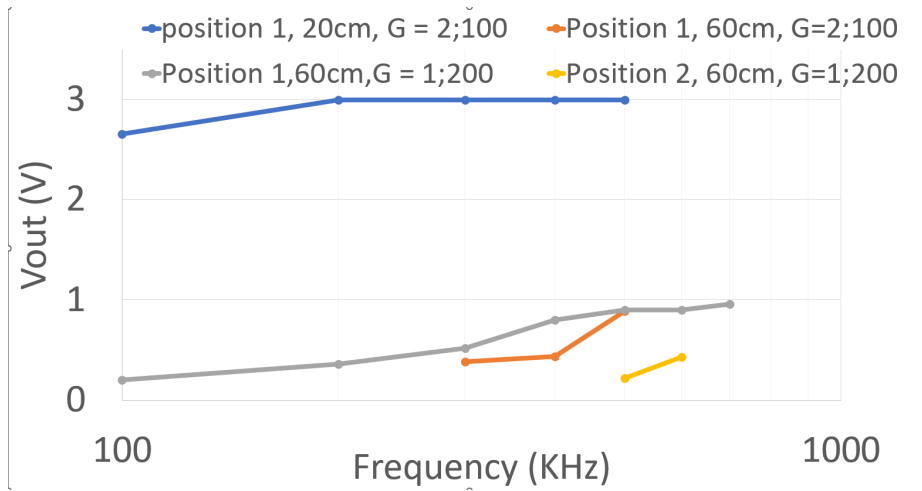


Fig. 13. Output Rx signal amplitude on a Bluefin tuna in different position

The total average consumption is 315 μ A and the current consumption peak are 15mA for Tx and 2,7mA for the Rx.

The GC transceiver specifications are notably the transmission frequency and distance. The system allows to communicate from 1kHz to 800kHz. The maximum frequency is limited by the In Amp GBW. As a consequence, it should be difficult to implement applications such as endoscopy which needs to transmit at MHz frequency to enable video transmission. In order to upgrade the proposed architecture in terms of maximum transmission frequency, it becomes mandatory to replace the In Amp by a more complex amplification stage made of more components and an additional supply voltage which would induce a higher consumption and size. Two In Amps have been tested. It appears that the INA823 has a larger GBW while the AD623 has a better amplification.

5 Conclusion and perspectives

We have shown that it is possible to propose a fully miniaturized architecture for GC only with discrete components. Size and consumption depend only on desired frequency and data rate. The proposed architecture responds to a range of size, consumption and frequencies that has been validated in several experimental setting, demonstrating the feasibility of intra - extra body communication.

We assume that Tx consumption can be drastically reduced to few mA by redesigning the architecture. There are several redesign possibilities, such as removing the DDS to generate a single frequency signal using the micro-controller, switching-off a maximum number of components when there isn't any transmission or reception and transmission duration.

In order to increase the transmission distance, it becomes mandatory to implement a transmission protocol such as the promising DSSS DPSK. The implementation of Rx programmable gain could also permit to increase the transmission distance. As the living tissue conductivity increases with increasing frequency, we could expect a longer transmission distance while increasing the transmission frequency.

References

1. R. Noormohammadi, A. Khaleghi, I. Balasingham, Galvanic impulse wireless communication for biomedical implants, *IEEE Access* 9 (2021) 38602–38610. doi:10.1109/ACCESS.2021.3064206.
2. A. K. Teshome, B. Kibret, D. T. H. Lai, A review of implant communication technology in wban: Progress and challenges, *IEEE Reviews in Biomedical Engineering* 12 (2019) 88–99. doi:10.1109/RBME.2018.2848228.
3. D. Ahmed, G. Fischer, J. Kirchner, Simulation-based models of the galvanic coupling intra-body communication, 2019 *IEEE Sensors Applications Symposium (SAS)* (2019) 1–6.
4. T. Leng, Z. Nie, W. Wang, F. Guan, L. Wang, A human body communication transceiver based on on-off keying modulation, in: *International Symposium on Bioelectronics and Bioinformatics 2011*, 2011, pp. 61–64. doi:10.1109/ISBB.2011.6107645.

5. M. D. F. L. Zhiying Chen, Yueming Gao, A circuit-coupled fem model with considering parasitic capacitances effect for galvanic coupling intrabody communication, *Progress In Electromagnetics Research C* 106 (2020) 17–27. doi:10.2528/PIERC20072701.
6. W. K. Chen, Z. L. Wei, Y. M. Gao, L. Vasić, M. Cifrek, M. I. Vai, M. Du, S. H. Pun, Design of galvanic coupling intra-body communication transceiver using direct sequence spread spectrum technology, *IEEE Access* 8 (2020) 84123–84133. doi:10.1109/ACCESS.2020.2991206.
7. J. Bae, H.-J. Yoo, The effects of electrode configuration on body channel communication based on analysis of vertical and horizontal electric dipoles, *IEEE Transactions on Microwave Theory and Techniques* 63 (4) (2015) 1409–1420. doi:10.1109/TMTT.2015.2402653.
8. M. J. Park, T. Kang, I. G. Lim, K.-I. Oh, S.-E. Kim, J.-J. Lee, H.-I. Park, Low-power, high data-rate digital capsule endoscopy using human body communication, *Applied Sciences* 8 (9) (2018). doi:10.3390/app8091414. URL <https://www.mdpi.com/2076-3417/8/9/1414>
9. E. Detrez, V. Kerzérho, M.-M. Belhaj, A. Vergnet, H. de Verdal, T. Rouyer, S. Bonhommeau, A. Lamlih, M. Julien, F. Ben Ali, M. Renovell, S. Bernard, F. Soulier, Study differentiating fish oocyte developmental stages using bioimpedance spectroscopy, *Aquaculture* 547 (2022) 737396. doi:<https://doi.org/10.1016/j.aquaculture.2021.737396>. URL <https://www.sciencedirect.com/science/article/pii/S0044848621010590>